NUMERICAL MULTISCALE METHODS FOR COUPLED OSCILLATORS

GIL ARIEL*, BJORN ENGQUIST†, AND RICHARD TSAI‡

Abstract. A multiscale method for computing the effective slow behavior of a system of weakly coupled nonlinear planar oscillators is presented. The oscillators may be either in the form of a periodic solution or a stable limit cycle. Furthermore, the oscillators may be in resonance with one another and thereby generate some hidden slow dynamics. The proposed method relies on correctly tracking a set of slow variables that is sufficient to approximate any variable and functional that are slow under the dynamics of the ODE. The technique is more efficient than existing methods and its advantages are demonstrated with examples. The algorithm follows the framework of the heterogeneous multiscale method.

Key words. Multiscale computation, nonlinear oscillators, resonance, phase locking, slow variables

AMS subject classifications. 65L05,34E13

1. Introduction. Ordinary differential equations (ODEs) with highly oscillatory periodic solutions prove to be a challenging field of research from both the analytic and numerical points of view [15, 16]. Several different numerical approaches have been suggested, each appropriate to some class of ODEs. Dahlquist laid down the fundamental work for designing linear multistep methods [4, 5, 6, 7] and studied their stability properties. Stiff problems with fast transients can be optimally solved by implicit schemes [4, 18, 22]. The Chebyshev methods [1, 24] as well as the projective integrator approach [13] provide stable and explicit computational strategies for this class of problems in general. Chebyshev methods are also efficient with problems that have a cascade of different scales which are not necessarily well separated. For harmonic oscillatory problems, traditional numerical approaches attempt to either filter out or fit fast oscillations to some known functions in order to reduce the complexity, e.g. [12, 23, 30], or use some notion of Poincaré map to determine slow changes in the orbital structure [14, 27]. A general class of approaches aiming at Hamiltonian systems are geometric integration schemes that preserve a discrete version of certain invariance. We refer the readers to [17] and [25] for an extensive list of literature. Many of the schemes specialized for finite dimensional mechanical systems can be conveniently derived from the view point of variational integrator; see the review paper [26]. In certain applications, special considerations are given to the expensive cost of evaluating non-local potentials in large systems, see e.g. the impulse method and its derivatives [25]. For a recent review on numerical methods for highly oscillatory systems see [3].

We refer to a pair (x, y) as an oscillator if the trajectory $(x(t), y(t))$ is either periodic or approaches a stable periodic limit cycle. The period of an oscillator is denoted T_0.

*Department of Mathematics, The University of Texas at Austin, Austin, TX, 78712, USA (ariel@math.utexas.edu).

†Department of Mathematics, The University of Texas at Austin, Austin, TX, 78712, USA (engquist@math.utexas.edu).

‡Department of Mathematics, The University of Texas at Austin, Austin, TX, 78712, USA (ytsai@math.utexas.edu).

One typical example is the Van der Pol oscillator [31],

$$\ddot{x} = -x + \nu(1 - x^2)\dot{x}, \tag{1.1}$$

for some $\nu > 0$. Equation (1.1) has a unique and stable limit cycle that tends to the circle $x^2 + \dot{x}^2 = 4$ in the limit $\nu \to 0$. Another type of oscillators arise when a system of ODEs has a family of periodic solutions.

In this paper we propose a numerical multiscale scheme for the initial value problems in which different oscillators are coupled weakly. The period of each oscillation is taken to be proportional to a small parameters $\epsilon \ll 1$. The effect of the coupling only becomes significant on a longer time scales. We are particularly interested in resonance or synchronization effects. Consequently, we assume that the frequencies of the uncoupled oscillators are commensurable, i.e. linearly independent over the rationals.

Let $\{(x_k, y_k)\}_{k=1}^{l}$ denote a set of l oscillators with $x_k, y_k \in \mathbb{R}$. We consider ODE systems in singular perturbation form

$$\epsilon\dot{\mathbf{x}} = f(\mathbf{x}) + \epsilon g(\mathbf{x}), \qquad \mathbf{x}(0) = \mathbf{x}_0, \tag{1.2}$$

where $0 < \epsilon \leq \epsilon_0$ and $\mathbf{x} = (x_1, y_1, x_2, y_2, \ldots, x_l, y_l)$. It is further assumed that the solution of (1.2) remains in a domain $\mathcal{D}_0 \subset \mathbb{R}^{2l}$, that is bounded independent of ϵ for all $t \in [0, T]$, $T < \infty$ and independent of ϵ. For fixed ϵ and initial condition $\mathbf{x}_0$, the solution of (1.2) is denoted $\mathbf{x}(t; \epsilon, \mathbf{x}_0)$. For brevity we will write $\mathbf{x}(t)$ whenever it is clear what the values for ϵ and $\mathbf{x}_0$ are. On short time scales of order ϵ, the term $\epsilon g(\mathbf{x})$ can be neglected. However, on longer time scales which are independent of ϵ, this perturbation may accumulate to an important contribution that cannot be ignored.

One of the main difficulties in numerical integration of (1.2) using explicit methods is that stability and accuracy requirements severely restrict the usable step size. This generally implies that the computational complexity for integrating (1.2) over a time T independent of ϵ is at least of the order of ϵ^{-1}. This is the motivation for multiscale numerical schemes that take advantage of the separation between time scales in the problem. The new schemes proposed in this paper generalize those in [2] to systems of nonlinear oscillators. The computational cost of our proposed schemes are sublinear in the frequency of the oscillators. Furthermore, it can be applied to problems for which specialized algorithms such as the exponential integrators [17, 20] do not apply, or do not yield efficient approximations.

The various types of oscillators make a general method difficult. As a recourse, we first describe the main idea behind our algorithm and then apply it to several examples involving different types of oscillators. An important component in our approach is to identify a set of functions of $\mathbf{x}$ that are slow with respect to the dynamics of (1.2), i.e., the time derivatives of these functions are uniformly bounded with a constant that is independent of ϵ along the trajectories of (1.2). We classify these functions as amplitudes and the relative phases between the oscillators. We generally refer to them as the slow variables of the system. The ODE (1.2) is then integrated using the framework of the heterogeneous multiscale method (HMM) [9, 10, 11] — a Macro-solver integrates the effective, but generally unknown evolution equation for the slow variables under the dynamics of (1.2), where the rate of change for these slow variables are computed by a micro-solver that integrates the full ODE (1.2) for short time segments.

For convenience, Section 2 reviews the main results and algorithm proposed in [2] and [11]. Section 3 describes a method for applying the HMM algorithm to systems of weakly coupled oscillators. Several examples are studies in Section 4 including harmonic, Volterra-Lotka and relaxation oscillators. The Volterra-Lotka example admits a family of periodic solutions that correspond to some constants of motion. On the other hand, in the relaxation oscillator example trajectories rapidly approach a stable limit cycle. We conclude in Section 5.

2. The HMM scheme. In this section we summarize the main results of [2] and [11]. We begin by analyzing how the slow aspects of a multiscale ODE can be identified and separated from the fast one by using a convenient system of coordinates. Then, an algorithm for approximating and evolving these slow aspects is reviewed.

2.1. Fast and slow dynamics. We study the long time properties of (1.2) by separating the fast and slow constituents of the dynamics and investigating the interactions between these constituents and their collective effective behavior. We say that a real valued smooth function (variable) $\alpha(\mathbf{x})$ is slow with respect to (1.2) if there exists a non-empty open set $\mathcal{A} \subset \mathbb{R}^d$ such that

$$\max_{\mathbf{x}_0 \in \mathcal{A}, t \in \mathcal{I}, \epsilon \in (0,\epsilon_0]} \left| \frac{d}{dt} \alpha(\mathbf{x}(t;\epsilon,\mathbf{x}_0)) \right| \leq C_0, \tag{2.1}$$

where C_0 is a constant that is independent of ϵ and $\mathcal{I} = [0,T]$. Otherwise, $\alpha(\mathbf{x})$ is said to be fast. Similarly, we say that a quantity or constant is of order one if it is bounded independent of ϵ in $\mathcal{A}$. We typically consider functions that are independent of ϵ. For integrable Hamiltonian systems, the action variables are indeed slow variables.

Of course, any function of slow variables is also slow. Therefore, it is reasonable to look for variables which are functionally independent, i.e., a vector of slow variables $\xi = (\xi_1(\mathbf{x}), \ldots, \xi_r(\mathbf{x}))$ such that $\nabla\xi_1(\mathbf{x}), \ldots, \nabla\xi_r(\mathbf{x})$ are linearly independent in $\mathcal{A}$. Since r is bounded by the dimension, d, it is useful to look at a set with a maximal number of functionally independent slow variables. Augmenting the slow variables with $d-r$ fast ones $z = (z_1, \ldots, z_{d-r})$ such that $\partial(\xi, z)/\partial\mathbf{x}$ is non-singular in $\mathcal{A}$, one obtains a local coordinate systems, i.e., a chart of the states space. We will refer to a chart in which a maximal number of coordinates is slow as a maximal slow chart for $\mathcal{A}$ with respect to the ODE (1.2). Covering the set $\mathcal{D}_0$ by maximal slow charts we obtain a maximal slow atlas for $\mathcal{D}_0$.

A second type of slow behavior, referred to as slow observables, are integrals of the trajectories. For example, for any integrable function $\alpha(\mathbf{x}, t)$, the integral

$$\tilde{\alpha}(t) = \int_0^t \alpha(\mathbf{x}(s), s) ds \tag{2.2}$$

is slow since $|d\tilde{\alpha}/dt| \leq C$ for some constant $C > 0$ Additional slow observables can be obtained using convolution with a compactly supported kernels, as explained at the end of this Section.

One of the main difficulties is, that it is often not clear a priori what are the slow variables and observables of interest for a specific problem. For this reason, we take a wide approach and require that our algorithm approximates all variables and observables which are slow with respect to the ODE. To see how it is possible, let $(\xi, \phi) \in \mathbb{R}^d$

denote a slow chart with slow coordinates $\xi \in \mathbb{R}^r$ and let $\alpha(\mathbf{x}) : \mathbb{R}^d \to \mathbb{R}$ a slow variable. Then, by the maximality of the chart, there exists a function $\tilde{\alpha} : \mathbb{R}^r \to \mathbb{R}^d$ such that $\alpha(\mathbf{x}) = \tilde{\alpha}(\xi(\mathbf{x}))$, otherwise, $\alpha(\mathbf{x})$ can be added as an additional coordinate. Hence, if the values of ξ along the trajectories of (1.2) are approximated accurately, then the values of *any* other smooth slow variable are automatically approximated. Furthermore, it is not necessary to know $\tilde{\alpha}$ since all points $\mathbf{x}$ which correspond to the same ξ yield the same value of $\alpha(\mathbf{x})$. In [2] we prove that approximation of ξ is also sufficient to approximate all slow observables of the types described above.

Construction of our multiscale algorithm is done in three stages. The first required identification of a maximal slow chart or atlas (ξ, ϕ) which needs to be defined in a neighborhood of the trajectory. Locally, any coordinates system on a manifold that is perpendicular to $f(\mathbf{x})$ can serve as a maximal slow chart. However, extending a chart to include the full trajectory is more complicated. This is done in [2] for the case in which the leading order term in (1.2) is linear, $f(\mathbf{x}) = A\mathbf{x}$. The main purpose of this paper is to offer a similar construction for some cases in which the solutions are still periodic even though $f(\mathbf{x})$ may not be linear.

The second stage is to establish the existence of an effective evolution equation for the slow variables $\xi(\mathbf{x}(t))$ under the flow of (1.2). In all the examples discusses in this paper, we find that the only fast coordinate is equivalent to rotation on the unit circle with constant velocity, i.e., $\phi \in \mathbb{S}^1$. This case is quite general since many weakly perturbed integrable systems in resonance fall into this category. Then, an averaging principle can be used to prove that for small ϵ, $\xi(\mathbf{x}(t; \epsilon, \mathbf{x}_0))$ is well approximated in $\mathcal{I}$ by an effective equation of the form

$$\dot{\xi} = F(\xi), \quad \xi(0) = \xi(\mathbf{x}_0). \tag{2.3}$$

See [2, 29] for details. The requirement that (ξ, ϕ) is a maximal slow chart is critical for the derivation of (2.3). Without it, there is no guaranty that the right hand side of the averaged equation does not depend on additional slow variables which may be hidden or unknown.

The effective equation (2.3) may not be available as an explicit formula. Instead, the idea behind the HMM algorithm is to evaluate $F(\xi)$ by numerical solutions of the original ODE (1.2) on significantly reduced time intervals. In this way, the HMM algorithm approximates an assumed effective equation whose form is typically unknown. This strategy is advantageous if $F(\xi)$ can be approximated efficiently. Finally, the third stage of the process is to construct such an algorithm. This is explained below in Section 2.2.

In [2] we present both analytic and numerical methods for finding a maximal slow chart in a neighborhood of the trajectories in the case in which $f(\mathbf{x})$ is linear, i.e., $f(\mathbf{x}) = A\mathbf{x}$ and A is a diagonalizable matrix whose eigenvalues have non-positive real parts. It is then proved that the slow atlas can be described using a single chart which consists of the following slow variables:

- Slow variables that correspond to a basis of the Null space of A.
- Amplitudes of oscillators (or rather square of), which are quadratic functions of $\mathbf{x}$.
- The relative phase between each pair of oscillators which correspond to some specific coupling of different oscillators through initial conditions. If the ratio between the frequencies of two oscillators is a rational number, then this relative phase can be defined by a specific polynomial in $\mathbf{x}$.

A simple example is the following system described by

$$\epsilon\dot{\mathbf{x}} = \begin{pmatrix} 0 & 1 & 0 & 0 & 0 \\ -1 & 0 & 0 & 0 & 0 \\ 0 & 0 & 0 & 2 & 0 \\ 0 & 0 & -2 & 0 & 0 \\ 0 & 0 & 0 & 0 & 0 \end{pmatrix} \mathbf{x} + \epsilon g(\mathbf{x}), \tag{2.4}$$

where $\mathbf{x} = (x_1, y_1, x_2, y_2, x_3)$. Here (x_1, y_1) and (x_2, y_2) are harmonic oscillators with frequencies $1/2\pi$ and $1/\pi$, respectively. One verifies that x_3 is slow and that the square amplitudes, $I_1 = x_1^2 + y_1^2$ and $I_2 = x_2^2 + y_2^2$, are slow. In addition, the cubic polynomial $J_1 = x_1^2 x_2 + 2x_1 y_1 y_2 - y_1^2 x_2$ is also slow. This is verified by differentiating $J_1(\mathbf{x}(t))$ with respect to time. The polynomial J_1 is related to the relative phase between the two harmonic oscillators, a quantity that varies slowly in time.

The main purpose of this paper is to extend these ideas to a wider class of ODEs. We find that the components of slow charts can be interpreted as some generalized concepts of amplitudes and relative phases.

2.2. The algorithm. Suppose $\xi = (\xi_1(\mathbf{x}), \ldots, \xi_r(\mathbf{x}))$ are the slow variables in a slow atlas for (1.2). The system is integrated using a two level algorithm, each level corresponding to a different time scale. The first is a Macro-solver, which integrates the effective equation (2.3) for the slow variables ξ. The second level is a micro-solver that is invoked whenever the Macro-solver needs an estimate of $F(\xi)$. The micro-solver computes a short time solution of (1.2) using suitable initial data. Then, the time derivative of ξ is approximated by

$$\dot{\xi}(t) \sim \langle \dot{\xi}(t) \rangle_\eta = \int_{-\eta/2}^{\eta/2} \dot{\xi}(t+\tau) K_\eta(t-\tau) d\tau, \tag{2.5}$$

where, $K_\eta(\cdot)$ denotes a smooth averaging kernel with support on $[-\eta/2, \eta/2]$. Note that $\dot{\xi}$ is not necessarily slow. However, it is bounded independent of ϵ. The properties of averaging with respect to a kernel will be reviewed shortly.

Once time derivatives are approximated, the system needs to be evolved in a way that is consistent with (2.5). For example, a step $\mathbf{x}(t+H) = \mathbf{x}(t) + \Delta\mathbf{x}$, correct to second order in H, is to take the least squares solution of the linear system

$$\Delta\mathbf{x} \cdot \nabla\xi_k(\mathbf{x}(t)) = H \langle \dot{\xi}_k(t) \rangle_\eta, \; k = 1, \ldots, r.$$

Higher order methods are developed in [2].

To better explain the algorithm, denote the Macro-solver sample times by $t_0, \ldots, t_N$, $N = T/H$, and its output at corresponding times by $\mathbf{x}_0, \ldots, \mathbf{x}_N$. At the n-th Macro-step, the micro-solver can be implemented using any scheme with step-size h and initial condition $\mathbf{x}(t_n) = \mathbf{x}_n$. It integrates the full ODE both backwards and forward in time to approximate the solution in $[t_n - \eta/2, t_n + \eta/2]$. The structure of the algorithm, depicted in Figure 2.1, is as follows.

1. Initial conditions: $\mathbf{x}(0) = \mathbf{x}_0$ and $n = 0$.
2. Force estimation:
   (a) micro-simulation: Solve (1.2) in $[t_n - \eta/2, t_n + \eta/2]$ with initial conditions $\mathbf{x}(t_n) = \mathbf{x}_n$.

(b) Averaging: approximate $\dot{\xi}_k(t_n)$ by $\langle \dot{\xi}_k(t_n) \rangle_\eta$.

3. Macro-step (forward Euler example):
   $\mathbf{x}_{n+1} = \mathbf{x}_n + HF_n$, where F_n is the least squares solution of the linear system

$$F_n \cdot \nabla \xi_k(\mathbf{x}_n) = \langle \dot{\xi}_k(t_n) \rangle_\eta, \quad k = 1 \dots r$$

4. $n = n + 1$. Repeat steps (2) and (3) to time T.

The averaged time derivative of ξ_k, $\langle \dot{\xi}_k \rangle_\eta$, can be calculated using either the chain rule as $\dot{\xi}_k = \nabla \xi_k \cdot \dot{\mathbf{x}} = \nabla \xi_k \cdot (f(\mathbf{x}) + \epsilon g(\mathbf{x}))$, or using integration by parts. The scheme described above can be generalized to Macro-solvers with higher order accuracy.

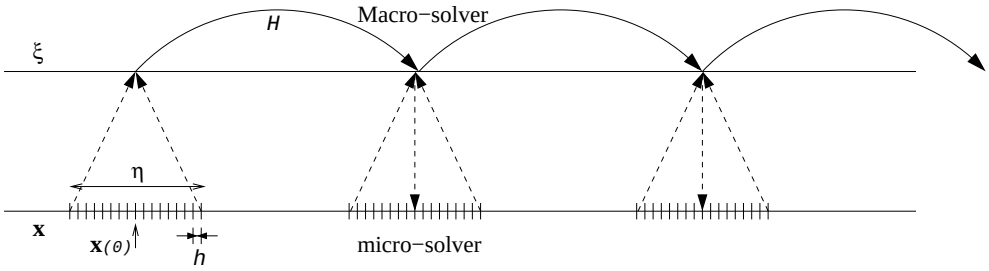

FIG. 2.1. *The cartoon depicts the time steps taken by the HMM scheme. At the n-th macro step, a micro-solver with step size h integrates (1.2) to approximate* $\mathbf{x}(t)$ *in a time segment* $[t_n - \eta/2, t_n + \eta/2]$. *This data is used to calculate* $\langle \xi(\mathbf{x}(t)) \rangle_\eta$. *Then, the Macro-solver takes a big step of size* HF_n, *where* F_n *is consistent with* $\langle \dot{\xi}_k \rangle_\eta$, *i.e.,* $F_n \cdot \nabla \xi_k = \langle \dot{\xi}_k \rangle_\eta$ *for all slow variables* ξ_k *in the maximal slow chart.*

Let $K(\cdot)$ denote a smooth kernel function with support on $[-1, 1]$ with unit mass, $\int_{-1}^{1} K(\tau) d\tau = 1$, and zero average, $\int_{-1}^{1} K(\tau) \tau d\tau = 0$. For simplicity, we assume that $K(\cdot)$ is symmetric with respect to its mid-point. For example, the following smooth exponential kernel was found useful:

$$K(t) = Z^{-1} \exp\left(-\frac{5}{4} \frac{1}{(t-1)(t+1)} \right), \tag{2.6}$$

for $t \in [-1, 1]$ and zero otherwise. Here, Z is a normalization constant. For $\eta > 0$ let,

$$K_\eta(\tau) = \frac{1}{\eta} K(\frac{1}{\eta} \tau). \tag{2.7}$$

We will take η to be ϵ dependent such that $\epsilon < \eta \ll 1$. The convolution of a function $a(t)$ with K_η is denoted as (recall (2.5))

$$\langle a(t) \rangle_\eta = \int_{-\eta/2}^{\eta/2} a(t + \tau) K_\eta(t - \tau) d\tau. \tag{2.8}$$

Typically, the fast dynamics in equations such as (1.2) is one of two types. The first consists of modes that are attracted to a low dimensional manifold in ϵ-time scale. These modes are referred to as transient or dissipative modes. The second type consists of oscillators with constant or slowly changing frequencies. Dissipative modes can be relaxed using asymmetric kernels while averaging of oscillatory modes filters out high frequency oscillations. The errors introduced by the averaging are estimated in [2]. Asymmetric kernels can also be used in order to obtain an improved accuracy.

Finally, the stability of the algorithm is related to integration of the approximate effective equation for the slow variables, $\dot{\xi} = \langle \dot{\xi}(\mathbf{x}(t)) \rangle_\eta$ using the Macro-solver of choice. Additional details can be found in [10] and [11].

3. Slow charts for coupled oscillators. In this section we outline a method for constructing slow charts for weakly coupled oscillators. A few specific examples are detailed in section4. For simplicity, we consider a system of two planar oscillators, $z, \gamma \in \mathbb{R}^2$, of the form

$$\begin{aligned} \epsilon \dot{z} &= f(z) \\ \epsilon \dot{\gamma} &= g(\gamma), \end{aligned} \tag{3.1}$$

where the trajectory $(z(t; z_0), \gamma(t; \gamma_0)) \in \mathbb{R}^2 \times \mathbb{R}^2$ is either periodic or approaches a stable periodic limit cycle. In addition, consider the perturbed systems

$$\begin{aligned} \epsilon \dot{\tilde{z}} &= f_\epsilon(\tilde{z}, \tilde{\gamma}) = f(\tilde{z}) + \epsilon h(\tilde{z}, \tilde{\gamma}) \\ \epsilon \dot{\tilde{\gamma}} &= g_\epsilon(\tilde{z}, \tilde{\gamma}) = g(\tilde{\gamma}) + \epsilon k(\tilde{z}, \tilde{\gamma}). \end{aligned} \tag{3.2}$$

We would like to study the effective behavior of the coupled system (3.2), in particular the effective influence of the perturbative coupling. This could be done using some generalized notions of amplitude and relative phase to form slow charts in the state space.

Suppose that, in the limit $\epsilon \to 0$, the trajectory of each oscillator approaches a stable periodic limit cycle. Two possibilities may occur [19, 21, 29, 32]. First, the limit cycle may be attractive, in which case any trajectory that starts close enough will be asymptotically close to it. Second, there may a continuous one parameter family of periodic orbits. In either case, one can often use this parameter to describe the closeness of the trajectory to the limit cycle [19]. In the first case, the parameter is a dissipative, "fast" variable. In the second case it is slow. We think of this parameter as some generalized amplitude, in the sense that it identifies the periodic limit cycle of the oscillators. See, for example the discussion on the Van der Pol oscillator in [19]. The generalized amplitudes of the two oscillators are denoted I_1 and I_2, respectively.

3.1. Slowly changing observables along the trajectories. We observe that along each trajectory of (3.2), a slow variable defines a slowly changing quantity ϑ. First, consider the unperturbed equation (3.1) and a slow variable $\alpha(z, \gamma)$. We denote

$$\frac{d}{dt}\alpha(z(t), \gamma(t)) = \frac{1}{\epsilon}(\nabla_z \alpha|_{z(t),\gamma(t)} \cdot f + \epsilon \nabla_\gamma \alpha|_{z(t),\gamma(t)} \cdot g) =: \phi_\alpha^{f,g}(t; z_0, \gamma_0), \tag{3.3}$$

where ∇_z and ∇_γ denote the gradients with respect to z and γ, respectively. Because $\alpha(z, \gamma)$ is slow, we have that $|\phi_\alpha^{f,g}(t; z_0, \gamma_0)| \leq C_1$. If this bound is valid for $0 < \epsilon \leq \epsilon_0$, then $\nabla_z \alpha \cdot f = 0$. Next, consider the perturbed equation (3.2). We may directly consider integrating a slow observable $\vartheta(t)$ satisfying

$$\frac{d}{dt}\vartheta = \phi_\alpha^{f_\epsilon, g_\epsilon}(t; y_0), \quad \vartheta(0) = \vartheta_0. \tag{3.4}$$

Notice that

$$\phi_\alpha^{f_\epsilon, g_\epsilon} = \frac{1}{\epsilon}(\nabla_z \alpha|_{z(t),\gamma(t)} \cdot f_\epsilon + \epsilon \nabla_\gamma \alpha|_{z(t),\gamma(t)} \cdot g_\epsilon) = \nabla_z \alpha|_{z(t),\gamma(t)} \cdot h + \nabla_\gamma \alpha|_{z(t),\gamma(t)} \cdot k.$$

Hence, $\vartheta(t)$ is slowly varying on a $\mathcal{O}(1)$ time scale.

3.2. Relative phase defined by time. We first consider the unperturbed system (3.1). Time may be used to defined what the phase of the trajectory of an oscillator means. Suppose that there exists two functions $\tau_z(z)$ and $\tau_\gamma(\gamma)$ such that $\tau_z(z(t)) = \epsilon^{-1}t + c_0$ and $\tau_\gamma(\gamma(t)) = \epsilon^{-1}t + c_1$. Then, the relative phase between the $z(t)$ and $\gamma(t)$ can be defined as $\theta(z(t), \gamma(t))$, where

$$\theta(z, \gamma) := \tau_z(z) - \tau_\gamma(\gamma).$$

We see that $\theta(z(t), \gamma(t))$ is constant which is independent of ϵ. For the coupled system (3.2), we find that the quantity defined by

$$\frac{d}{dt}\vartheta := \frac{d}{dt}\theta(\tilde{z}(t), \tilde{\gamma}(t)) = \frac{1}{\epsilon}\nabla\theta \cdot \begin{pmatrix} f(\tilde{z}) + \epsilon h(\tilde{z}, \tilde{\gamma}) \\ g(\tilde{\gamma}) + \epsilon k(\tilde{z}, \tilde{\gamma}) \end{pmatrix} = \nabla\theta \cdot \begin{pmatrix} h(\tilde{z}, \tilde{\gamma}) \\ k(\tilde{z}, \tilde{\gamma}) \end{pmatrix} \tag{3.5}$$

measures how the relative phase between $\tilde{z}$ and $\tilde{\gamma}$ is changing under the coupling.

In oscillatory systems, inverse functions such as τ_z and τ_γ cannot usually exist globally. To define the relative phase this way, we have to allow for the possibility of using a collection of locally defined inverse functions whose domains collectively cover a given periodic orbit of the problem. Consider the case in which two patches $\tau_z^{(1)}$ and $\tau_z^{(2)}$ are needed. We can glue the two patches together via a partition of unity $\{\phi_1, \phi_2\}$ supported on the domain of $\tau_z^{(1)}$ and $\tau_z^{(2)}$. Enforcing that the values of $\tau_z^{(1)}$ and $\tau_z^{(2)}$ are identical where they are both defined, we have that

$$\tau_z = \phi_1\tau_z^{(1)} + \phi_2\tau_z^{(2)}$$

and

$$\nabla\tau_z = \phi_1\nabla\tau_z^{(1)} + \phi_2\nabla\tau_z^{(2)}.$$

Performing similar procedures to obtain $\nabla\tau_\gamma$, the relative phase can then be defined as (3.5).

For many problems, even though the inverse function τ does not exist globally, we can obtain a smooth, globally well-defined gradient from the locally defined inverses. In this case, we may employ (3.3) to integrate a slow quantity. For example, the derivative of $\arctan(z)$ is defined on the whole real line. Similarly, on the complex plane, the derivative of the arg function is defined everywhere except at the origin. In the latter case, the integral of $\tau_z(z)$ and $\tau_\gamma(\gamma)$ over closed orbits can be thought of as the winding numbers around $z = 0$ and $\gamma = 0$, respectively, and (3.3) defines a continuous $\theta(t)$ on a Riemann sheet.

4. Examples. For simplicity, we consider two coupled planar oscillators, (x_1, y_1) and (x_2, y_2). Generalizations to systems with a larger number of oscillators can be performed in a similar fashion.

4.1. Harmonic oscillators. We begin with the simple case in which $f(\mathbf{x})$ is linear, i.e. $f(\mathbf{x}) = A\mathbf{x}$ for some diagonalizable matrix whose eigenvalues are purely imaginary. Such systems were already considered in [2]. Here we apply the alternative approach proposed in Section 3 so that the effect of the coupling with fully nonlinear

oscillators can be studied systematically via the notion of relative phase. Without loss of generality, we assume that the ODE is in diagonalized form

$$\begin{aligned} \epsilon \dot{x}_k &= \omega_k y_k + \epsilon g_k(\mathbf{x}) \\ \epsilon \dot{y}_k &= -\omega_k x_k + \epsilon h_k(\mathbf{x}), \end{aligned} \tag{4.1}$$

for $k = 1 \dots l$, where $\omega_k \neq 0$ and $\mathbf{x} = (x_1, y_1, \dots, x_l, y_l)$. Note that g_k and h_k are not necessarily linear.

Under the dynamics of (4.1), it it easy to identify the r slow variables relating to the square of the amplitudes:

$$I_k(\mathbf{x}) = x_k^2 + y_k^2, \tag{4.2}$$

for all $k = 1 \dots l$. In [2], it was shown that if the frequencies $\{\omega_k/2\pi\}_{k=1}^l$ are rationally related, i.e., ω_k/ω_j is rational for all k, j, then there exists additional $l-1$ polynomials $J_1(\mathbf{x}), \dots, J_{l-1}(\mathbf{x})$ that are slow. The variables J_k correspond to a notion of relative phases between the oscillators. Adding a single additional fast variable, ϕ, yields a maximal slow chart with respect to (4.1), denoted $(I_1, \dots, I_l, J_1, \dots, J_{l-1}, \phi)$. Following our previous notations, $r = 2l - 1$.

Consider a harmonic oscillator on the unit circle

$$\begin{aligned} X(t) &= \sin(\omega t + \phi_0) \\ Y(t) &= \cos(\omega t + \phi_0). \end{aligned} \tag{4.3}$$

$X(t)$ and $Y(t)$ thus satisfy

$$\begin{aligned} \dot{X} &= \omega Y \\ \dot{Y} &= -\omega X, \;\; X(0)^2 + Y(0)^2 = 1. \end{aligned} \tag{4.4}$$

Time t can be uniquely defined up to a constant term using the arctan function:

$$t = \omega_k^{-1} \left[\arctan(\frac{Y}{X}) - \phi_0 \right]. \tag{4.5}$$

Furthermore, the derivative of arctan is globally defined for all values of X and Y. Thus, $\arctan(Y/X)$ is a good candidate to find time. From our discussion in Section 3, for the system (4.1), the relative phase between the two oscillators can be defined as

$$\theta(x_1, y_1, x_2, y_2) := \omega_1^{-1} \arctan(\frac{y_1}{x_1}) - \omega_2^{-1} \arctan(\frac{y_2}{x_2}). \tag{4.6}$$

Hence, θ represents the angle, or phase difference between two points, (x_1, y_1) and (x_2, y_2), when written in the polar coordinates. If we evaluate θ along the trajectories of the solutions of (4.1), we have that

$$\frac{d}{dt}\theta(\mathbf{x}(t)) = \nabla\theta \cdot \dot{\mathbf{x}} = \frac{g_1 y_1 - x_1 h_1}{\omega_1 I_1} - \frac{g_2 y_2 - x_2 h_2}{\omega_2 I_2}, \;\; \text{and} \;\; |\frac{d}{dt}\theta(\mathbf{x}(t))| \leq C_0. \tag{4.7}$$

Hence $\theta(\mathbf{x})$ is slow with respect to (4.1).

Since the inverse tangent function is only defined locally, so is $\theta(\mathbf{x})$. Nonetheless, as discussed in Section 3.1, $\vartheta(t) = \int_0^t (d/d\tau)\theta(\mathbf{x}(\tau))d\tau$ defines a continuously changing quantity or observable.

As an example, consider a Van der Pol oscillator (1.1) with $\nu = \epsilon$, weakly coupled to a harmonic oscillator with frequency $(2\pi)^{-1}$:

$$\begin{aligned} \epsilon \dot{x}_1 &= y_1 + \epsilon A x_2, \\ \epsilon \dot{y}_1 &= -x_1 + \epsilon(1 - x_1^2) y_1, \\ \epsilon \dot{x}_2 &= y_2 + \epsilon \omega y_2, \\ \epsilon \dot{y}_2 &= -x_2 + \epsilon \omega x_2. \end{aligned} \tag{4.8}$$

with initial conditions $x_1 = y_1 = x_2 = 1$ and $y_2 = 0$. The parameter A is a coupling constant and is independent of ϵ. With $A = 0$, (x_1, y_1) is a Van der Pol oscillator (1.1) with $\nu = \epsilon$ and (x_2, y_2) is a harmonic oscillator with frequency $(1 + \epsilon\omega)/(2\pi)$. Hence, the difference between the frequencies of the two oscillators is of order ϵ. For $A \neq 0$ the two oscillators are coupled weakly. It follows from our discussion above that I_1, I_2 and θ given by (4.2) and (4.6) are slow variables with respect to (4.8).

The algorithm described in Section 2.2 was implemented using the slow chart ξ with $\epsilon = 10^{-4}$ and $\omega = 10$. Other parameters are $H = 0.5$, $h = \epsilon/15$, $\eta = 25\epsilon$ and (2.6) as a kernel. Both micro and Macro solvers employ a fourth order Runge-Kutta scheme. We compare results for $A = 0$ and $A = 10$. Figure 4.1 depicts the time evolution of the amplitude of the Van der Pol oscillator, $I_1 = x_1^2 + y_1^2$. In order to observe the effect of the relative phase, we plot in Figure 4.2 the values of x_1 and x_2 during three different runs of the micro-solver. In Figure 4.2a, $A = 0$ and the two oscillators are decoupled. We see that the two oscillators slowly drift out of phase due to the slightly different frequencies. With $A = 10$ the oscillators are coupled and maintain a constant relative phase. The phenomenon of phase locking, (also called entrainment or synchronization) is well known for nonlinear oscillators [16, 28].

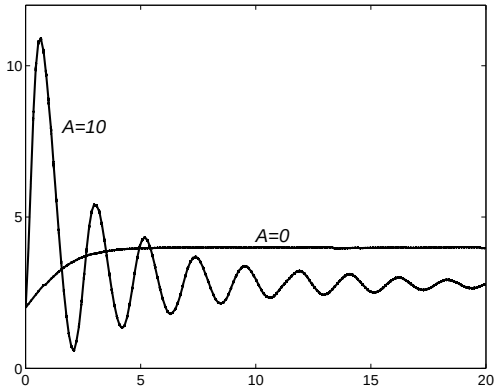

FIG. 4.1. *The amplitude of the Van der Pol oscillator described by (4.8). $A = 0$: decoupled and $A = 10$: coupled to a harmonic oscillator with a slightly different frequency.*

4.2. The Volterra-Lotka oscillator. In this section we consider the Volterra-Lotka oscillator, which is treated as a benchmark case for oscillators that admit a conserved quantity. The Volterra-Lotka oscillator is given by the ODE

$$\begin{aligned} \dot{x} &= x(1 - \nu^{-1} y) \\ \dot{y} &= \nu^{-1} y(x - 1), \end{aligned} \tag{4.1}$$

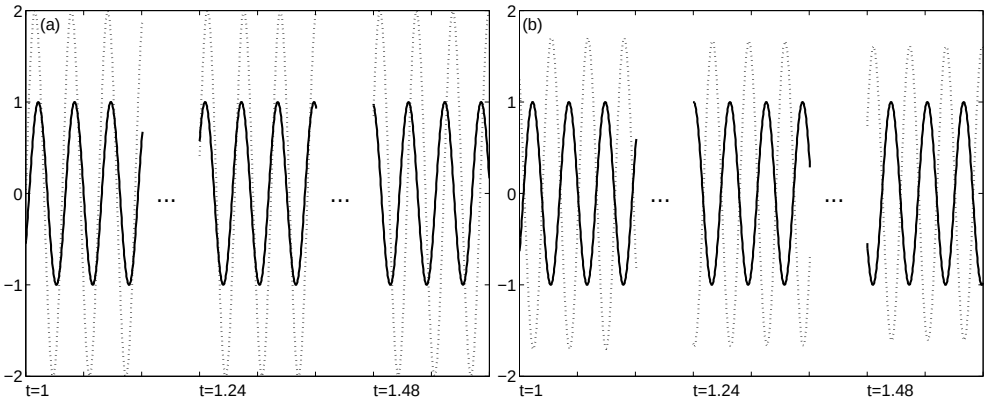

FIG. 4.2. *The phase of the Van der Pol and harmonic oscillators described by (4.8). (a) $A = 0$: decoupled, and (b) $A = 10$: coupled to a harmonic oscillator with a slightly different frequency. Dotted line: $x_1(t)$ — Van der Pol oscillator, solid line: $x_2(t)$ — harmonic. The two oscillators are synchronized when coupled.*

where $0 < \nu \ll 1$ is a small parameter. Equation (4.1) admits a family of periodic solutions with period $T_0(\nu)$ that can be parametrized according to the initial conditions $0 < x(0) < 1$ and $y(0) = 1$. An example of such periodic trajectories is depicted in Figure 4.3.

It can be verified that

$$I_{VL}(x, y) = x - \ln x + y - \nu \ln y \tag{4.2}$$

is a conserved quantity along each periodic solution of equation (4.1), and it may play the role of the oscillator's amplitude.

Each periodic orbit can be divided into the union of two continuous open segments which are joined by two points, (x_I, ν) and (x_{II}, ν), where x_I,and x_{II} are the solutions of $I_{VL}(x, \nu) = C_0$. We denote the first segment by Γ_I which consists of a relatively slow movement close to the x-axis. The second segment, Γ_{II}, corresponds to the trajectory along the upper arc depicted in Figure 4.3. In a duration proportional to ν, the solution goes through the upper arc and comes downs to the first segment. The trajectory goes from one segment to the other whenever its y component equals ν, at which location, $\dot{x} = 0$. Away from $y = \nu$, $\dot{x} > 0$ when the trajectory is on Γ_I and $\dot{x} < 0$ on Γ_{II}. This suggests that an inverse function mapping the trajectory to some reference time coordinate can be defined separately on each segment:

$$\tau_I(x(t), y(t)) = t, \text{ for } (x(t), y(t)) \in \Gamma_I$$

and

$$\tau_{II}(x(t), y(t)) = t + C_{II}, \text{ for } (x(t), y(t)) \in \Gamma_{II}.$$

Hence, for $(x, y) \in \Gamma_I$,

$$\frac{\partial \tau_I(x, y)}{\partial x}\dot{x} + \frac{\partial \tau_I(x, y)}{\partial y}\dot{y} = \frac{1}{\epsilon}. \tag{4.3}$$

Further more, it is convenient to take $\nabla \tau_I \cdot \nabla I_{VL} = 0$.

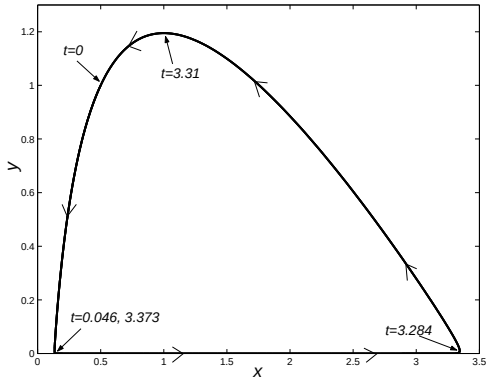

FIG. 4.3. *The trajectory of the Volterra-Lotka oscillator (4.1) with* $\nu = 0.01$, $x(0) = 0.5$ *and* $y(0) = 1$.

Away from the turning points at $y = \nu$, the gradient for $\tau_2(x, y)$ are exactly the same as that of $\tau_1(x, y)$. Denoting $\mathbf{1}_\Gamma$ as the indicator function of the set Γ we formally define τ and $\nabla\tau$ by

$$\tau = \mathbf{1}_{\bar{\Gamma}_I}(x, y)\tau_I(x, y) + \mathbf{1}_{\Gamma_{II}}(x, y)\tau_{II}(x, y),$$

and

$$\nabla\tau = \mathbf{1}_{\bar{\Gamma}_I}(x, y)\nabla\tau_I(x, y) + \mathbf{1}_{\Gamma_{II}}(x, y)\nabla\tau_{II}(x, y).$$

Let $(X_1(t), Y_1(t))$ denote a periodic solution of (4.1) and $(X_2(t), Y_2(t))$ denote an unperturbed harmonic oscillator with frequency ω. Similar to the approach described in Section 4.1, we define

$$\theta(X_1, Y_1, X_2, Y_2) = \tau(X_1, Y_1) - \omega^{-1}\arctan(\frac{Y_2}{X_2}). \tag{4.4}$$

From the discussion of Section 3.2, the slow observable ϑ defined by

$$\frac{d}{dt}\vartheta = \nabla\theta \cdot \begin{pmatrix} \dot{X}_1 \\ \dot{Y}_1 \\ \dot{X}_2 \\ \dot{Y}_2 \end{pmatrix}$$

is a well-defined continuous function of time, which is related to the relative phase between the oscillators.

Now, consider the weak coupling of a Volterra-Lotka and a harmonic oscillator:

$$\begin{aligned} \epsilon\dot{x}_1 &= x_1(1 - \nu^{-1}y_1) + \epsilon g_1(\mathbf{x}), \\ \epsilon\dot{y}_1 &= \nu^{-1}y_1(x_1 - 1) + \epsilon h_1(\mathbf{x}), \\ \epsilon\dot{x}_2 &= \omega y_2 + \epsilon g_2(\mathbf{x}), \\ \epsilon\dot{y}_2 &= -\omega x_2 + \epsilon h_2(\mathbf{x}). \end{aligned} \tag{4.5}$$

Thus, as we argued in Section 3.1, along each trajectory of (4.6) we can define the relative phase between the two oscillators as a slowly changing observable satisfying

$$\frac{d}{dt}\vartheta = \left(\nabla\theta \cdot (\epsilon^{-1} f)\right)|_{\gamma(t)}, \quad \vartheta(0) = 0,$$

where f denotes the right hand side of (4.6).

As an example, the HMM algorithm was applied to (4.6) with $\epsilon = 10^{-5}$, $\nu = 0.2$, $g_1 = y_2^2$, $h_1 = 0$, $g_2 = 0$ and $h_2 = x_1$. The frequency of the harmonic oscillator is taken to be close to that of the Volterra-Lotka one, $\omega = 3.77/2\pi$. The singularity at $y_1 = \nu$ is not problematic since $\nabla\theta\cdot\dot{\mathbf{x}}$ is integrable. Hence, we apply a cutoff around $|y_1 - \nu| < 10^{-4}$, which introduces an additional error evaluated by changing the cutoff value. Improved accuracy can be obtained by using methods such as Padé approximations in order to integrate over the problematic region. Additional parameters are $H = 0.25$, $\eta = 40$ (which is about 11 periods) and the integration kernel is (2.6). The micro-solver is a fourth order Runge-Kutta scheme with step size $h = 0.03\epsilon$. The Macro-solver is the midpoint rule. In addition, as explained in Section 3.2, we made sure that the macro-step is not taken with y_1 values close to ν. Figure 4.4 compares the solution of the amplitudes $I_1(x_1, y_1) = I_{VL}(x_1, y_1)$ and $I_2 = x_2^2 + y_2^2$ obtained by the HMM algorithm (plus signs) with that of the fourth order Runge-Kutta method (solid line) with the same step size $h = 0.03\epsilon$.

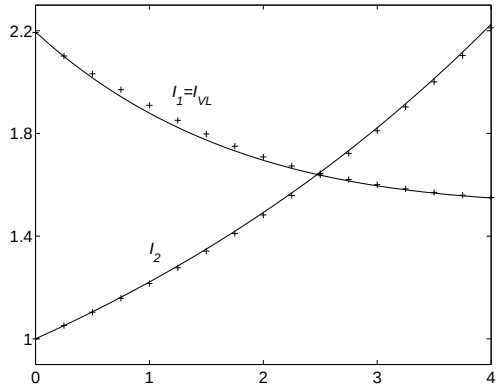

FIG. 4.4. *The amplitude of the Volterra-Lotka oscillator, $I_1 = I_{VL} = x_1 - \ln x_1 + y_1 - \nu \ln y_1$, and the harmonic oscillator, $I_2 = x_2^2 + y_2^2$. Fourth order Runge-Kutta (solid line) compared to HMM (plus signs).*

4.3. Relaxation oscillators. Consider the following example system suggested by Dahlquist et. al. [8]

$$\begin{aligned} \dot{x} &= -1 - x + 8y^3 \\ \dot{y} &= \nu^{-1}(-x + y - y^3), \end{aligned} \tag{4.1}$$

where $\nu \ll 1$ is a small parameter. The dynamics of (4.1) has a limit cycle that is defined by the cubic polynomial $x = y - y^3$ and the turning points $dx/dy = 0$ on it. The limit cycle consists of four parts, $\Gamma_{I,}$, Γ_{II}, Γ_{III}, and Γ_{IV}. Γ_I and Γ_{III} denote, respectively, the upper and lower branches of this cubic polynomial which are stable up to the turning points. For any initial condition, the solution of (4.1) is

attracted to one of the stable branches on an $O(\nu)$ time scale. The time derivative $\dot{x}$ stays positive when the trajectory is close to Γ_I and negative when close to Γ_{III}. Thus, trajectories of (4.1) move close to a branch until it becomes unstable. At this point the solution is quickly attracted to the other stable branch. During the transient states, the trajectories stay close to Γ_{II} and Γ_{IV}. The trajectory of the oscillator near the limit cycle is depicted in Figure 4.5. Van der Pol dubbed the name relaxation oscillators due to the fast relaxation process at the instabilities. We shall use the structure of this limit cycle to parametrize time.

The amplitude of the relaxation oscillator can be defined by some notion of distance between the trajectory and the limit cycle, for example, as the difference in the y coordinates of the trajectory and the limit cycle at some fixed x. This is effectively a particular realization of the Poincaré map with a transversal segment $x = const.$ Under the dynamics of (4.1), this distance converges to zero exponentially fast in a time scale of order ν. Hence, the amplitude of the oscillator can be considered a dissipative variable.

Next, we discuss how to define the phase of the oscillator. In order to do so, we need to make our description of the limit cycle more precise. As we alluded above, it consist of four parts: The vertical segments, Γ_{II} and Γ_{IV}, are defined by the intersections of $x = \pm 2\sqrt{3}/9$ and $x = y - y^3$:

$$\Gamma_{II} = \{(x, y) : x = \frac{2\sqrt{3}}{9}, y \in I_2\},$$

$$\Gamma_{IV} = \{(x, y) : x = -\frac{2\sqrt{3}}{9}, y \in I_4\},$$

where $I_2 = (b_2, 2\sqrt{3}/9)$ and $I_4 = (-2\sqrt{3}/9, b_4)$ are the intervals bounded by the two solutions of $y - y^3 = 2\sqrt{3}/9$ and $y - y^3 = -2\sqrt{3}/9$, respectively. Hence,

$$\Gamma_I = \{(x, y) : x = y - y^3, \frac{1}{\sqrt{3}} < y < b_4\},$$

$$\Gamma_{III} = \{(x, y) : x = y - y^3, b_2 < y < -\frac{1}{\sqrt{3}}\}.$$

We shall assume that the solution of (4.1) is already sufficiently close to the limit cycle Γ. Near either Γ_I or Γ_{III}, $x(t)$ is strictly monotone, therefore, away from a neighborhood of the two turning points, we define τ_I and τ_{II} to be the inverse function of $x(t)$ on these two branches. Again, we formally define

$$\tau(x, y) = \mathbf{1}_{\Gamma_I}\tau_I + \mathbf{1}_{\Gamma_{II}}\tau_I + \mathbf{1}_{\Gamma_{III}}\tau_{III} + \mathbf{1}_{\Gamma_{IV}}\tau_{IV}$$

and the gradient

$$\nabla\tau = \mathbf{1}_{\Gamma_I}\nabla\tau_I + \mathbf{1}_{\Gamma_{II}}\nabla\tau_{II} + \mathbf{1}_{\Gamma_{III}}\nabla\tau_{III} + \mathbf{1}_{\Gamma_{IV}}\nabla\tau_{IV}.$$

Finally, the phase is defined as the solution of

$$\frac{d}{dt}\vartheta = \nabla\tau \cdot f.$$

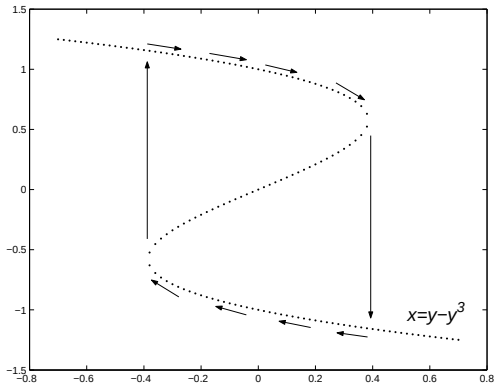

FIG. 4.5. *The trajectory and slow manifold of the relaxation oscillator (4.1).*

We use this strategy to study the following system in which a relaxation oscillator with $\nu = \epsilon$ is weakly coupled to a harmonic oscillator:

$$\begin{aligned} \epsilon \dot{x}_1 &= -1 - x_1 + 8y_1^3 + \epsilon A x_2 \\ \epsilon \dot{y}_1 &= \epsilon^{-1}(-x_1 + y_1 - y_1^3) \\ \epsilon \dot{x}_2 &= \omega_0 y_2 + \epsilon \omega y_2 \\ \epsilon \dot{y}_2 &= -\omega_0 x_2 + \epsilon \omega x_2. \end{aligned} \tag{4.2}$$

Since the relaxation from one stable branch to the other occurs on a $\mathcal{O}(\epsilon^2)$ time scale, we simply ignore effects of those terms related to Γ_{II} and Γ_{IV} for convenience of computation. We define the interior of Γ_I and Γ_{III}:

$$\tilde{\Gamma}_I = \{(x,y) : x = y - y^3, \frac{1}{\sqrt{3}} + C_0\epsilon < y < b_4 - C_0\epsilon\},$$

$$\tilde{\Gamma}_{III} = \{(x,y) : x = y - y^3, b_2 + C_0\epsilon < y < -\frac{1}{\sqrt{3}} - C_0\epsilon\}.$$

We can formally define

$$\nabla\tilde{\tau} = \mathbf{1}_{\tilde{\Gamma}_I}\nabla\tau_I + \mathbf{1}_{\tilde{\Gamma}_{III}}\nabla\tau_{III},$$

where

$$\nabla\tau_I = \nabla\tau_{III} = \begin{pmatrix} (-1 - x_1 + 8y_1^3)^{-1} \\ 0 \end{pmatrix}.$$

The relative phase between the (x_1, y_1) and (x_2, y_2) is then given by

$$\theta(x_1, y_1, x_2, y_2) = \tilde{\tau}(x_1) - \frac{1}{\omega_0}\arctan(\frac{y_2}{x_2}).$$

As an example, we take $\omega_0 = 2\pi/T_0$, $T_0 = 0.28416$ is the angular velocity of the decoupled (x_1, y_1) oscillator. The initial conditions are $x_1 = 0$, $y_1 = -1$, and $x_2 =$

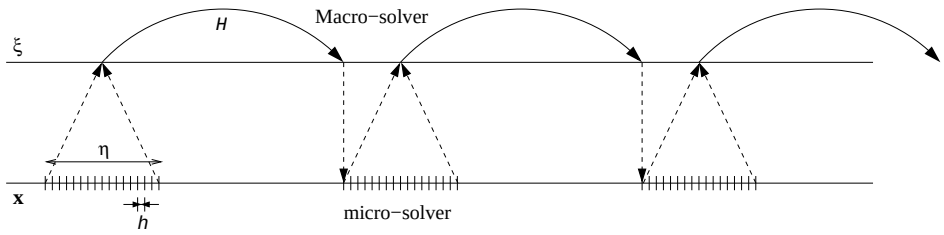

FIG. 4.6. *An asymmetric HMM for problems involving transients.*

$y_2 = 1/\sqrt{2}$. The parameter A is a coupling constant and is independent of ϵ. With $A = 0$, (x_1, y_1) is the relaxation oscillator (4.1) and (x_2, y_2) is a harmonic oscillator with angular velocity $\omega_0 + \epsilon\omega$. Hence, the frequencies of the two oscillators are close. For $A \neq 0$ the two oscillators are coupled weakly. The dynamics of (4.3) evolves on three time scales. The fastest scale, of order ϵ^2, is the relaxation time of the relaxation oscillator between stable branches. On an intermediate time scale of order ϵ, the coupling between the oscillators is negligible. The coupling becomes significant on a longer $\mathcal{O}(1)$ time scale. We apply HMM to take advantage of the scale separation between the two slowest modes.

The slow variables for (4.3) can be taken to be the amplitude of the harmonic oscillator, $I_2 = x_2^2 + y_2^2$, and the relative phase $\theta(\mathbf{x})$, which is well-defined in this example. Away from turning points, these variables describe a two dimensional slow manifold. Recall that the amplitude of the relaxation oscillator is dissipative.

The algorithm described in Section 2.2 was implemented using the above slow variables with $\epsilon = 10^{-4}$ and $\omega = 10$. The micro-solver, integrating the full system (4.3) was implemented using a forth order Runge-Kutta scheme with variable step size in order to speed up integration along the stable branches of the limiting cycle. Hence, our scheme operates on three time scales: ϵ^2, ϵ and 1. The Macro-solver uses a forward Euler scheme plus projection of the (x_2, y_2) oscillator onto the unit circle. Additional parameters are $H = 0.25$ and $\eta = 25\epsilon$. Due to the dissipative nature of the fast oscillations, the micro-solver only integrates the system forward in time and the resulting algorithmic structure is shown in Figure 4.6. Finally, it is important that macroscopic steps are not taken too close to the boundary of a chart, particularly if the boundary corresponds to a turning point of the trajectory. This can be avoided by running the micro-solver to time $\eta + T_0$, and then choosing a sub-segment of length η with a convenient mid-point for taking the macro-step.

We compare results for $A = 0$ and $A = 40$. Figure 4.2 depicts the values of x_1 and x_2 during three different runs of the micro-solver. In Figure 4.7a, $A = 0$ and the oscillators are decoupled. We see that the two oscillators slowly drift out of phase due to the slight difference in oscillator frequencies. With $A = 40$ the oscillators are coupled and maintain a constant relative phase. Figure 4.8 depicts the solution of (4.3) with $\omega_0 = 4\pi/T_0$, i.e, the frequency of the harmonic oscillator is slightly different than twice the frequency of the relaxation oscillator. With $A = 40$ the relaxation oscillator is synchronized with exactly half the frequency of the harmonic one. This phenomenon is referred to 1-2 entrainment or resonance.

5. Conclusion. Previously in [2], we have proposed an approach for decomposing a vector field into its fast and slow constituents using the concept of slow variables.

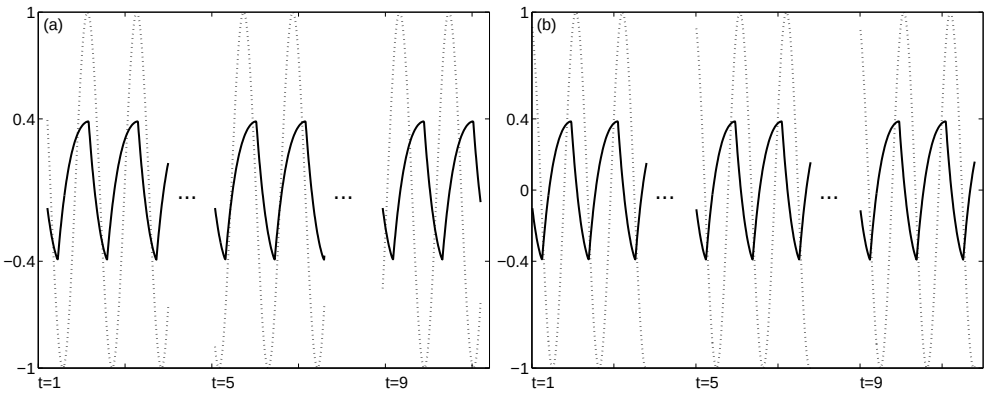

FIG. 4.7. *The phase of the relaxation and harmonic oscillators described by (4.3). (a) $A = 0$: decoupled, and (b) $A = 40$: coupled to a harmonic oscillator with a slightly different frequency. Dotted line: $x_2(t)$ — harmonic oscillator, solid line: $x_1(t)$ — relaxation. The two oscillators are synchronized when coupled.*

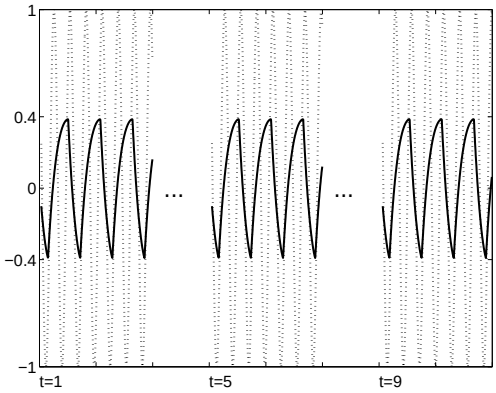

FIG. 4.8. *Example of 1-2 entrainment between a relaxation oscillator and a harmonic one. Dotted line: $x_2(t)$ — harmonic oscillator, solid line: $x_1(t)$ — relaxation.*

The decomposition is used in an algorithm that efficiently integrates the slow parts of the dynamics without fully resolving the fast parts globally in time. In this paper we further develop this idea and extend it to fully nonlinear oscillators. This includes oscillators which are very different in nature from harmonic oscillators. The slow variables are classified as amplitudes and relative phases, in analogy to corresponding variables for harmonic oscillators. The notion of relative phase is defined by constructing inverse functions that maps the periodic orbits to time. Following the HMM framework, the time evolution of the slow variables in the coupled system is computed using on the fly short-time simulations of the full system. Thus, we are able to compute efficiently the slow behavior of the system using large time steps.

Acknowledgments. Support from NSF through Grant DMS-0714612 is gratefully acknowledged. We thank Nick Tanushev and Eric Vanden-Eijnden for useful suggestions, corrections and discussions. Tsai's research is partially supported by an Alfred P. Sloan Fellowship. Tsai and Engquist thank the Isaac Newton Institute for

Mathematical Sciences for hosting parts of this research. Tsai also thanks the National Center for Theoretical Sciences at Taipei.

REFERENCES

[1] A. Abdulle. Fourth order Chebyshev methods with recurrence relation. *SIAM J. Sci. Comput.*, 23(6):2041–2054 (electronic), 2002.

[2] G. Ariel, B. Engquist, and R. Tsai. A multiscale method for highly oscillatory ordinary differential equations with resonance. *Math. Comp.*, 2008. Accepted. A preprint is available as a UCLA CAM report.

[3] D. Cohen, T. Jahnke, K. Lorenz, and C. Lubich. Numerical integrators for highly oscillatory hamiltonian systems: A review. In *Analysis, Modeling and Simulation of Multiscale Problems*, pages 553–576. Springer Berlin Heidelberg, 2006.

[4] G. Dahlquist. Convergence and stability in the numerical integration of ordinary differential equations. *Mathematica Scandinavica*, 4:33–53, 1956.

[5] G. Dahlquist. Stability and error bounds in the numerical integration of ordinary differential equations. *Kungl. Tekn. Högsk. Handl. Stockholm. No.*, 130:87, 1959.

[6] G. Dahlquist. A special stability problem for linear multistep methods. *Nordisk Tidskr. Informations-Behandling*, 3:27–43, 1963.

[7] G. Dahlquist. Error analysis for a class of methods for stiff non-linear initial value problems. In *Numerical analysis (Proc. 6th Biennial Dundee Conf., Univ. Dundee, Dundee, 1975)*, pages 60–72. Lecture Notes in Math., Vol. 506. Springer, Berlin, 1976.

[8] G. Dahlquist, L. Edsberg, G. Skollermo, and G. Soderlind. Are the numerical methods and software satisfactory for chemical kinetics? In *Numerical Integration of Differential Equations and Large Linear Systems*, volume 968 of *Lecture Notes in Math.*, pages 149–164. Springer-Verlag, 1982.

[9] W. E. Analysis of the heterogeneous multiscale method for ordinary differential equations. *Commun. Math. Sci.*, 1(3):423–436, 2003.

[10] W. E and B. Engquist. The heterogeneous multiscale methods. *Commun. Math. Sci.*, 1(1):87–132, 2003.

[11] B. Engquist and Y.-H. Tsai. Heterogeneous multiscale methods for stiff ordinary differential equations. *Math. Comp.*, 74(252):1707–1742, 2003.

[12] W. Gautschi. Numerical integration of ordinary differential equations based on trigonometric polynomials. *Numerische Mathematik*, 3:381–397, 1961.

[13] C. W. Gear and I. G. Kevrekidis. Projective methods for stiff differential equations: problems with gaps in their eigenvalue spectrum. *SIAM J. Sci. Comput.*, 24(4):1091–1106 (electronic), 2003.

[14] C.W. Gear and K.A. Gallivan. Automatic methods for highly oscillatory ordinary differential equations. In *Numerical analysis (Dundee, 1981)*, volume 912 of *Lecture Notes in Math.*, pages 115–124. Springer, 1982.

[15] J. Grasman. *Asymptotic methods for relaxation oscillations and applications*, volume 63 of *Applied Mathematical Sciences*. Springer-Verlag, 1987.

[16] J. Guckenheimer and P. Holmes. *Nonliner oscillations, dynamical systems and bifurcations of vector fields*, volume 42 of *Applied Mathematical Sciences*. Springer-Verlag, 1990.

[17] E. Hairer, C. Lubich, and G. Wanner. *Geometric numerical integration*, volume 31 of *Springer Series in Computational Mathematics*. Springer-Verlag, Berlin, 2002. Structure-preserving algorithms for ordinary differential equations.

[18] E. Hairer and G. Wanner. *Solving ordinary differential equations. II*, volume 14 of *Springer Series in Computational Mathematics*. Springer-Verlag, 1996.

[19] M.W. Hirsch, S. Smale, and R. Devaney. *Differential equations, dynamical systems, and an introduction to chaos*. Academic Press, Boston, 2004.

[20] M. Hochbruck, C. Lubich, and H. Selhofer. Exponential integrators for large systems of differential equations. *SIAM J. Sci. Comp.*, 19:1552–1574, 1998.

[21] J. Kevorkian and J. D. Cole. *Multiple Scale and Singular Perturbation Methods*, volume 114 of *Applied Mathematical Sciences*. Springer-Verlag, New York, Berlin, Heidelberg, 1996.

[22] H.-O. Kreiss. Difference methods for stiff ordinary differential equations. *SIAM J. Numer. Anal.*, 15(1):21–58, 1978.

[23] H.-O. Kreiss. Problems with different time scales. In *Acta numerica, 1992*, pages 101–139. Cambridge Univ. Press, 1992.

[24] V. I. Lebedev and S. A. Finogenov. The use of ordered Čebyšhev parameters in iteration

methods. *Ž. Vyčisl. Mat. i Mat. Fiz.*, 16(4):895–907, 1084, 1976.

[25] B. Leimkuhler and S. Reich. *Simulating Hamiltonian dynamics*, volume 14 of *Cambridge Monographs on Applied and Computational Mathematics*. Cambridge University Press, 2004.

[26] J.E. Marsden and M. West. Discrete mechanics and variational integrators. *Acta Numerica*, pages 357–514, 2001.

[27] R.L. Petzold, O.J. Laurent, and Y. Jeng. Numerical solution of highly oscillatory ordinary differential equations. *Acta Numerica*, 6:437–483, 1997.

[28] A. Pikovsky, M. Rosenblum, and J. Kurths. Phase synchronization in regular and chaotic systems. *Int. J. Bifurcation and Chaos*, 10(10):2291–2305, 2000.

[29] J. A. Sanders and F. Verhulst. *Averaging Methods in Nonlinear Dynamical Systems*, volume 59 of *Applied Mathematical Sciences*. Springer-Verlag, New York, Berlin, Heidelberg, Tokyo, 1985.

[30] R.E. Scheid. The accurate numerical solution of highly oscillatory ordinary differential equations. *Mathematics of Computation*, 41(164):487–509, 1983.

[31] B. Van der Pol. On relaxation oscillations. *Phil. Mag. 2*, 2:978–992, 1926.

[32] F. Verhulst. *Nonlinear differential equations and dynamical systems*. Springer, Berlin, New York, 1996.